AIAA 92-0009
Resolution Characteristics of Holographic Particle Image Velocimetry

J. Scherer and L.P. Bernal
University of Michigan
Ann Arbor, MI

30th Aerospace Sciences Meeting & Exhibit
January 6-9, 1992 / Reno, NV

RESOLUTION CHARACTERISTICS OF HOLOGRAPHIC PARTICLE IMAGE VELOCIMETRY

J. Scherer[*] and L.P. Bernal[†]
The University of Michigan
Ann Arbor, MI 48109 - 2140

Abstract

The resolution characteristics of in-line holographic imaging systems for application to velocity field measurement in turbulent and other vortical flows has been investigated experimentally. It is shown that the diameter of seed particles strongly influences the maximum size of the test volume that can be used as well as the spatial resolution of the measurement. Velocity measurements in a vortex ring flow using a two-axis holographic recording system are reported. The spatial resolution of this system is approximately 1 *mm*.

1. Introduction

Holographic imaging of flow seeded with small particles can be a useful technique for velocity field measurement in turbulent and other vortical flows. Several investigators have reported velocity measurements using holographic techniques.[1,2] Two basic approaches have been proposed. In most cases in-line doubly exposed holograms of the seeded flow are obtained. The velocity is determined from the displacement of the particles on the reconstructed images. This approach is what we call Holographic Particle Image Velocimetry (HPIV) because it is a natural extension of planar Particle Image Velocimetry[3]. A second approach[4,5] is to obtain a temporal sequence of holograms. The velocity is determined by tracking individual particles as a function of time. The main advantage of HPIV compared to particle tracking techniques is that the particle displacement is determined by local analysis of the reconstructed images which results is reduced image processing requirements.

Turbulent flow measurement requires a large spatial dynamic range. This requirement becomes more severe as the Reynolds number is increased. A large spatial dynamic range requires imaging of very small particles in a large test volume. Research on in-line holographic imaging systems for particle size measurement has shown a limit of the test volume depth of 50 to 80 far field distances.[6,7] (The far field distance is defined here as d^2/λ where d is the diameter of the particle and λ is the wavelength of laser used to record the hologram.) The depth of field of the reconstructed particle images is of the order of one far field distance.[8] The depth of field os the particle image is a good measure of the spatial resolution of the velocity measurement. It follows that the resolution characteristics of the holographic imaging system can severely limit the spatial dynamic range of HPIV.

In this paper we examine experimentally the resolution characteristics of in-line holographic imaging systems. A two-axis holographic recording system designed for high resolution velocity field measurements is described. Finally, velocity measurements in a vortex ring flow obtained to demonstrate this HPIV system are reported.

2. Holographic Imaging

The dynamic range requirements of typical HPIV recording systems dictates that the hologram be positioned at a large distance from the particles. In this case the light intensity distribution on the hologram plane is given by Fraunhofer theory[9]

$$I = 1 - \frac{\pi d^2}{2\lambda z}\sin\left(\frac{\pi r^2}{\lambda z}\right)\left[\frac{2 J_1\left(\frac{\pi d r}{\lambda z}\right)}{\frac{\pi d r}{\lambda z}}\right] + \left[\frac{\pi d^2}{4\lambda z}\frac{2 J_1\left(\frac{\pi d r}{\lambda z}\right)}{\frac{\pi d r}{\lambda z}}\right]^2 ,$$

where I is the light intensity at a distance z from the center of the particle, and

$$r = \sqrt{x^2 + y^2}$$

is the radial distance measured from the optical axis. Typical intensity distributions on the hologram plane are plotted in Figure 1. Figure 1 (a) is for a Fraunhofer number $F = d^2/\lambda z = 0.058$ and Figure 1 (b) for $F = 0.003$. These values correspond to typical particle sizes and hologram positions used in the experiments. In these plots the radial distance r is normalized by the radius of the particle a. The high Fraunhofer number case
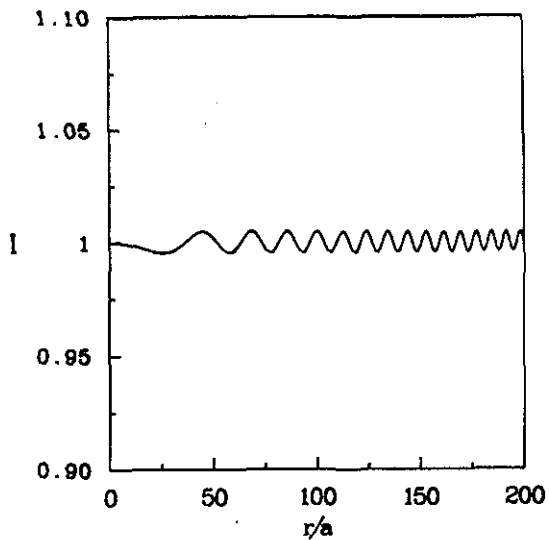
---

[*] Graduate Research Assistant.
[†] Associate Professor, Department of Aerospace Engineering. Member AIAA.
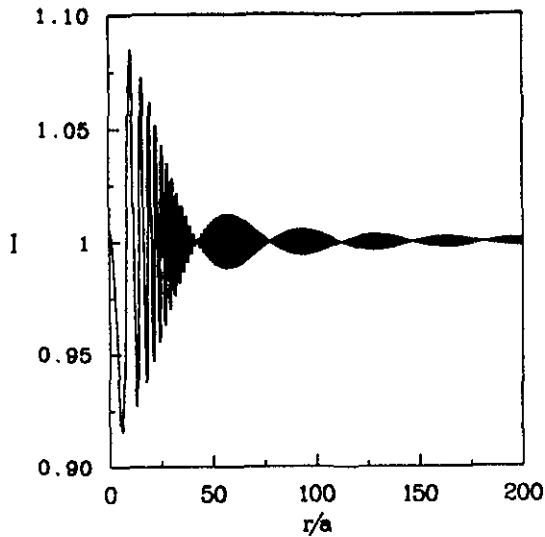
(a)

(b)

Figure 1. Intensity distribution on the hologram plane. (a) F = 0.058. (b) F = 0.003.

Figure 2. Fringe visibility as a function of the Fraunhofer number ——. Broken line: asymptotic behavior for F << 1.

shows a more complicated intensity pattern than the low Fraunhofer number case. In both cases the spatial frequency is not large and can be easily resolved by standard holographic plates. The amplitude of the oscillation is very small. As the Fraunhofer number is decreased the visibility of the fringes is reduced. This effect is illustrated in Figure 2 where the visibility parameter $V = I_{max} - I_{min}$ is plotted as a function of the Fraunhofer number. Here I_{max} and I_{min} are the maximum and minimum values, respectively, of the intensity distribution on the profiles. For small values of the Fraunhofer number V approaches the asymptotic behavior, $V = \pi F$, shown as a dotted straight line in Figure 2. The significance of this result is that for a fixed hologram distance, smaller particles produce a weaker fringe pattern. When the fringe visibility is comparable the noise level of the reference beam, it will not be possible to differentiate the reconstructed particle image from the background noise.
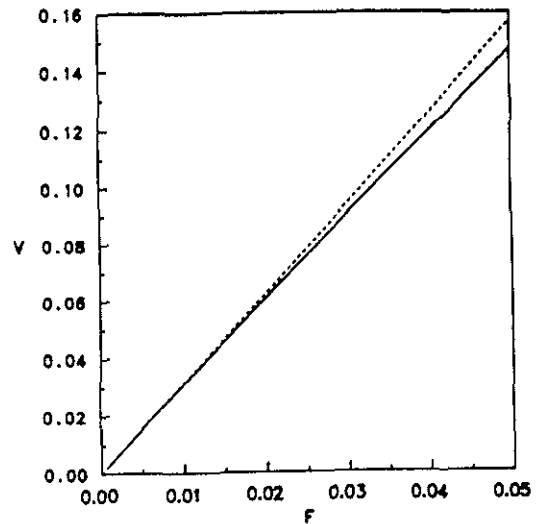
To document this effect in more detail a one-axis in-line holographic recording system identical to the one used in the velocity measurements was used to obtain holograms at several distances from the particles. These holograms were then used to measure the intensity distribution on the reconstructed images of the particles on the plane of best focus. The results are shown in Figure 3 and 4 for particles of 56 μm and 15μm diameter, respectively. As expected at the same hologram distance the 56 μm particles are better defined than the 15 μm particles. As the hologram distance is increased the contrast decreases until the particles can no longer be identified. These results are plotted in Figure 5 (a) and (b) for Fraunhofer numbers F = 0.0058 and 0.0030 respectively. At the larger Fraunhofer number the intensity distributions are very similar. At the low value, there is some discrepancies which are attributed to uncertainty in the measurement due to the very large hologram distances required for the 56 μm particles. It should be noted that the 15 μm particles give good contrast at F = 0.003. Based on these measurements we conclude that adequate particle images for HPIV are obtained for F ≥ 0.003. This correspond to a hologram distance of 333 far field lengths. This is much larger than the values reported for particle size measurements.[6,7] These results are not inconsistent since the images of the particles used for HPIV need not be as sharply defined as for size measurement..

Another important feature of in-line holographic imaging is the depth of field of the reconstructed particle images. The depth of field was determined by measurements of the screen intensity distribution on the reconstructed image of a 44 μm particle on a hologram for various distances, z, to the location of best focus. The results are presented in Figure 6. Figure 6 (a) is the screen intensity distribution as function of normalized radial distance. Figure 6 (b) is the screen intensity distribution as a function of axial distance to best focus. Note the different length scales of the two plots. The characteristic length scale in the radial
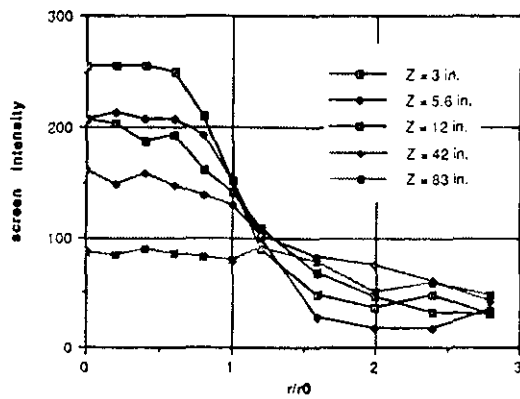
2

Figure 3. Screen intensity distribution on the plane of best focus of the reconstructed image of a 56 µm diameter particle for several hologram recording locations.

direction is the particle radius, and the characteristic length scale in the axial direction is the far field distance d^2/λ. A measure of the depth of field of the particle image is given by the broken lines in Figure 6 (b) spaced a distance $A = 4\ d^2/\lambda$ in the horizontal direction. Based on these results the depth of field of the particles is found $\pm 2\ d^2/\lambda$. This is twice the value proposed by Forbes and Kuehn.[8]
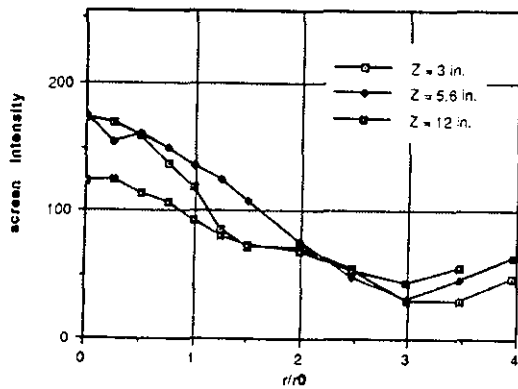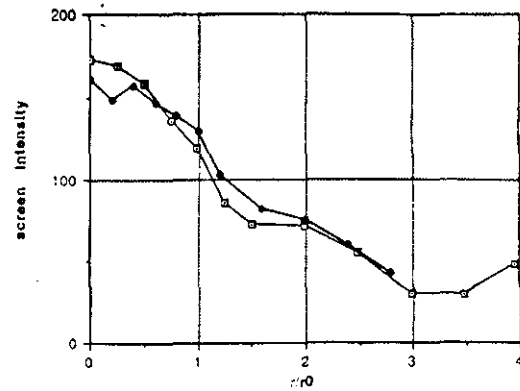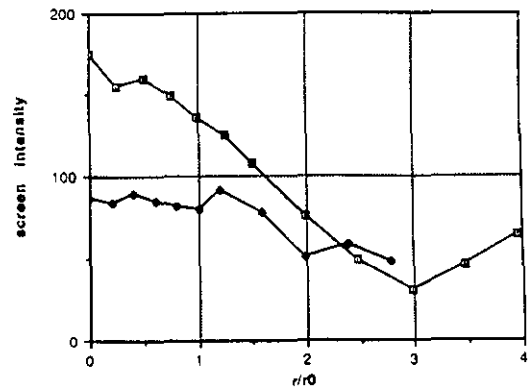

(a)

(b)

Figure 5. Screen intensity distribution on the plane of best focus. (a) F = 0.0058. (b) F = 0.003. ⌐15 µm particle, ⌐ 56 µm particle.

diagram of the hologram recording system is shown in Figure 7. This system uses a Copper Vapor Laser for the light source. A dichroic color separator is used to split the yellow and green lines one for each optical axis. Two similar optical systems are used to produce collimated beams of 150 mm diameter intersecting on the test area orthogonal to each other. The collimating optics of each beam incorporates a 100 µm spatial filter to improve the spatial coherence of the beam. Commercial holographic plates (100x125 mm) were used to record the holograms. They were positioned normal to the incoming collimated beams at approximately 200 mm from the center of the test area.

Figure 4. Screen intensity distribution on the plane of best focus of the reconstructed image of a 15 µm diameter particle for several hologram recording locations.

3. A two-axis HPIV recording system

The depth of field of the particle image limits the spatial resolution of the velocity measurement because it determines the distance between particles before they overlap. The depth of field also limits the accuracy of the displacement measurement in the direction of the optical axis. This second effect can be eliminated by using two orthogonal recording systems. Because of this a two-axis in-line holographic recording system was design and tested in a vortex ring flow field. A schematic

The vortex ring flow was produced in air using a loudspeaker covered by a thin steel plate having a 70 mm circular aperture. The flow was lightly seeded with glass microballoons having a specific gravity of 0.15 and a typical diameter of 15 - 20 µm. In order to insure that seeding particles were present in the vortical flow the vortex ring generator was covered and a signal applied to the loudspeaker to mix the seed particles. The flow inside the generator was allowed to decay before firing the vortex ring. As the ring propagated upwards through the test area, the Copper Vapor Laser was triggered with a pulse sequence consisting of two pulses followed by three pulses. This allowed the determination of the velocity magnitude and direction from the holograms. The entire firing sequence was automated in order to obtain consistent operation of the system.
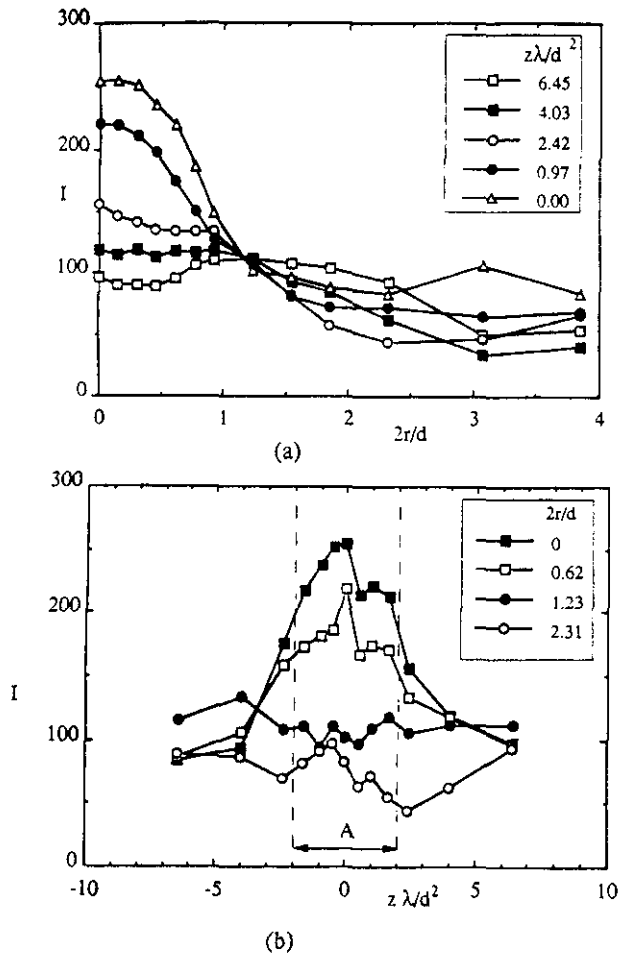
3

Figure 6. Screen intensity distribution for a 44 μm diameter particle as a function of radial location, (a); and axial location of the imaged plane, (b).

Figure 7. Schematic diagram of two-axis in-line holographic recording system.

The holograms were analyzed manually using a digital image analysis system. A x5 microscope objective was used to interrogate a small region of the flow. The velocity of the particles was determined by measuring the displacement on these images with a cursor. One hologram was automatically scanned in 5 mm intervals over a region one forth of the entire vortex ring. The displacement information on that hologram (two-components) was recorded. This information was then used to scan the second hologram to determine the remaining third component of the displacement. There is redundancy on the system in that one component of the displacement can be measured on both holograms. This information was used to verify that at every point the same particle pair was used to determine the velocity. It should be emphasized that in this system the velocity resolution is determined by the displacement of the particle between light pulses which is of the order of a few hundred microns much smaller than the depth of field of the particle image. Based on these results it is estimated that a spatial resolution of 1 *mm* can be obtained with this system.
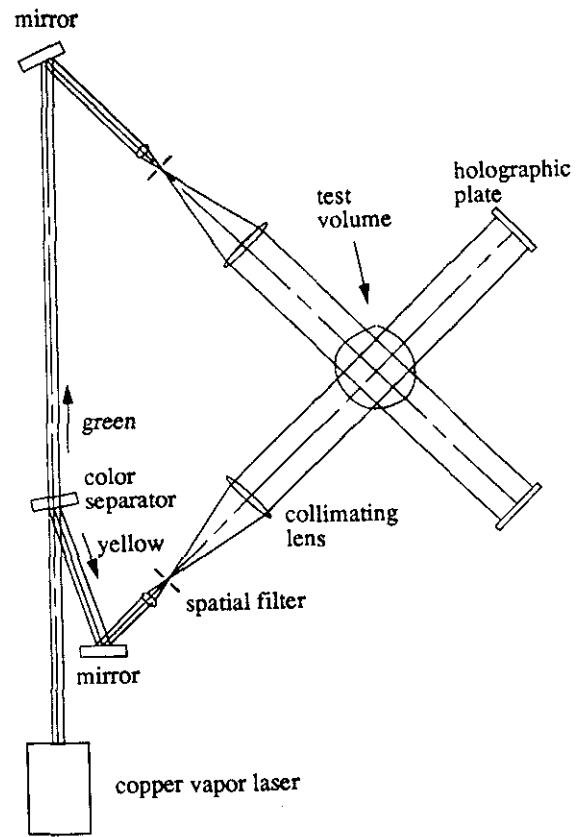
A vector plot of the velocity field in the vortex ring is shown in Figure 8. Because of the low seed concentration used the velocity was measured in ≈ 500 points only. No attempt was made to seed the fluid outside the vortex generator. Also the particles migrate away from the vortex core because of their density so that velocity measurements were not possible there. The circulation of the vortex ring estimated using these measurements is $\Gamma \approx 420 \ cm^2/s$.

4. Conclusions

The resolution characteristics of in-line holographic imaging systems was studied. A two-axis in-line holographic recording system was used to measure the velocity field in a vortex ring flow. The main conclusions of this study are:

- The maximum test volume depth was determined experimentally and found to be 300 far field lengths, d^2/λ.

- The resolution of the measurement is determined by the depth of field of the particle images which was found to be $\pm 2 \ d^2/\lambda$.

- A two-axis holographic recording system was demonstrated with velocity field measurements in a vortex ring flow. The spatial resolution of this system is of the order of 1 *mm*.
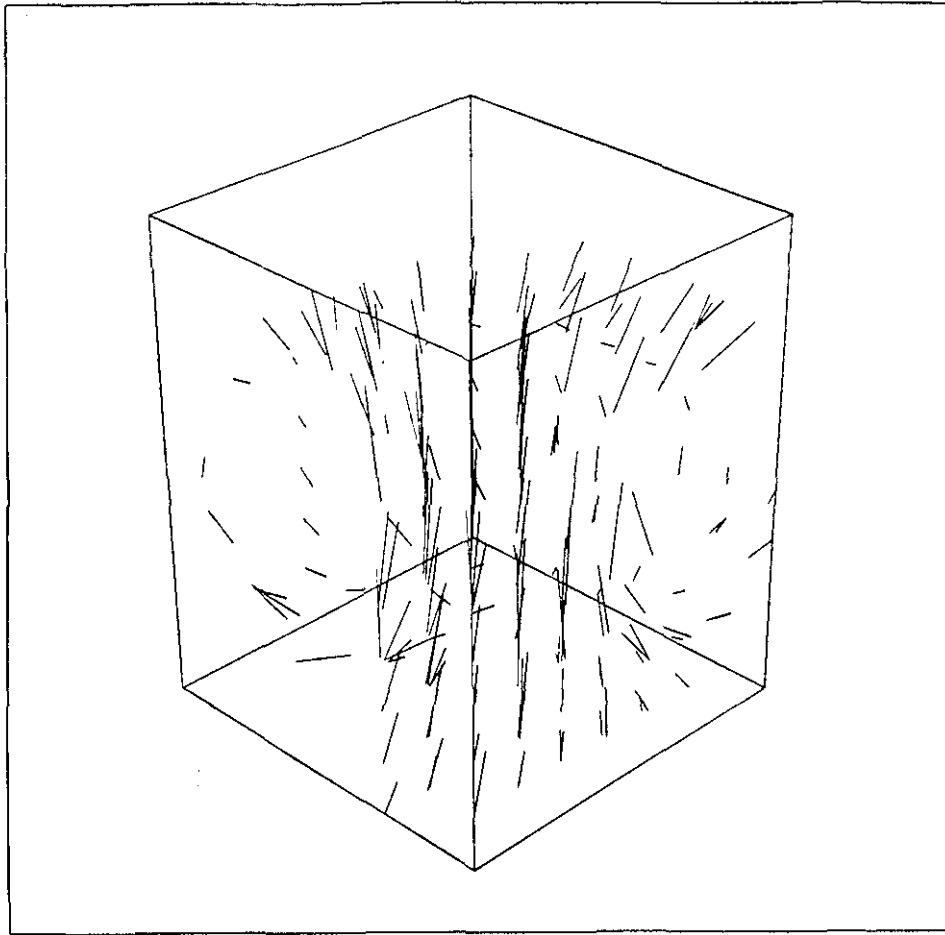
4

Figure 8.   Velocity vector plot of the measured velocity field in a vortex ring.

References

1. Trolinger, J. Farmer, W. and Beth, R., 1968 Multiple exposure holography of time varying three-dimensional fields, Applied Optics, 8, pp 1640-1641, 1969.

2. Schuster, P.R. and Wagner J.W., 1988, Holographic velocimetry for flow diagnostics, Exp. Mech., 28, pp 402-408.

3. Adrian, R.J. 1991 Particle-Imaging techniques for experimental fluid mechanics, Annu. Rev. Fluid Mech., 23, pp 261-304.

4. Weinstein, L.M., Beeler, G.B. and Linderman, A.M. 1985 High-Speed holocinematographic velocimeter for studying flow control physics, AIAA Paper 85-0526.

5. Ruff G.A., Bernal, L.P. and Faeth, G.M. 1990 High speed in-line holocinematography for dispersed-phase dynamics, Applied Optics, 29, pp 4544-4546.

6. Thompson, B.J., Ward, J.H. and Zinky, W.R. 1967 Application of hologram techniques for particle size analysis, Applied Optics, 6, pp 519-526.

7. Haussmann, G. and Lauterborn, W. 1980 Determination of size and position of fast moving gas bubbles in liquids by digital 3-D image processing of holograms reconstructions, Applied Optics, 19, pp 3529-3535.

8. Forbes, S.J. and Kuehn, T.H. 1990 In-Line particle holography using photographic threshold technique, FED-Vol. 95, ASME, pp 45-47.

9. Parrent, G.B.,Jr. and Thompson, B.J. 1964 On the Fraunhofer (far field) diffraction patterns of opaque an transparent objects with coherent background, Optical Acta, 11, pp 183-193.